Cold Regions Science and Technology 67 (2011) 24–30

Contents lists available at ScienceDirect

Cold Regions Science and Technology

journal homepage: www.elsevier.com/locate/coldregions

Wave scattering by an ice floe of variable thickness

Michael J.A. Smith, Michael H. Meylan *

Department of Mathematics, University of Auckland, Private Bag 92019, Auckland, New Zealand

ARTICLE INFO

Article history:
Received 7 September 2010
Accepted 3 March 2011

Keywords:
Ice floe
Elastic plate
Linear water waves

ABSTRACT

We present a solution for the problem of wave scattering by an ice floe of variable thickness, modeled as an elastic plate which floats with negligible submergence. The solution method is based closely on the equivalent problem for an ice floe of uniform properties. We show that the solution for an ice floe of variable properties can be calculated straightforwardly from the solution for a uniform floe by expressing the natural modes for the variable floe in terms of the modes for a uniform floe. This in turn allows us to use the solution for the added mass and damping which has been calculated for the constant floe, for the floe of variable properties. Numerical results for various non-uniform floes are given and the effect of realistic thickness variations is investigated.

1. Introduction

The standard model for a large ice floe is a floating elastic plate. The formulation of the problem and the first approximate numerical solutions were developed by Wadhams (1973, 1986). In two dimensions an exact solution method for this problem was not developed until the work of Fox and Squire (1994) for a semi-infinite floe and by Meylan and Squire (1994) for a finite floe. At the same time the equivalent model was solved motivated by engineering applications (Newman, 1994). Underlying all this is the assumption that the submergence of the plate is negligible, and we use this assumption in the present work. However, there have been some recent investigations into the effect of submergence (Williams and Porter, 2009; Williams and Squire, 2010). From this initial work, there have been two distinct motivations for the work on floating elastic plate, modeling ice floes and modeling *Very Large Floating Structures*. Many solution methods have been developed and we do not discuss these in detail, but instead refer readers to the excellent review articles by Watanabe et al. (2004) and Squire (2007). It is worth noting that almost all the work has been in the frequency domain, and the time-domain solution for floating elastic plates remains challenging. However, methods have been developed and a strong, but highly nontrivial connection exists between the solutions in the frequency domain and time domain (Hazard and Meylan, 2007; Meylan and Sturova, 2009).

The eigenfunction-matching method (Linton and McIver, 2002) provides one of the simplest methods to solve the problem for a uniform floating plate. This method was developed by Fox and Squire (1994) for a semi-infinite plate and it has been extended to circular plates (Peter et al., 2004), finite plates (Kohout et al., 2007) and multiple hinged plates (Kohout and Meylan, 2009) It has also been extended to submerged plates by Mahmood-ul-Hassan et al. (2009). There also exists another computationally simple solution method based on the Wiener–Hopf method (Balmforth and Craster, 1999; Chung and Fox, 2002; Tkacheva, 2001, 2004), which also works well for uniform plates. The Wiener–Hopf approach produces extremely efficient methods to calculate the solution, but this method is even more limited in the range of applications than the eigenfunction matching method (for example, it cannot be extended to three dimensions). Furthermore, the Wiener–Hopf method does not allow the consideration of non-uniform floes. The development of simple methods for non-uniform floes is an important area of current research, and methods have been developed by Williams and Squire (2004) and Bennetts et al. (2009).

The most straightforward method to solve for the linear response of a floating elastic plate is to generalize the method used to solve for a rigid body (Mei, 1989; Newman, 1977). In this method the body motion is solved for by an expansion in the rigid-body modes, and the effect of the fluid is found by solving an integral equation over the wetted surface of the body using Green's function for the fluid. To include the effect of the elasticity, the elastic as well as the rigid-body modes need to be included, and for this reason the solution method is sometimes referred to as the *generalized mode* method. Current computational methods allow for the solution of very complicated hydroelastic problems by this method, for example the response of a container ship (Hirdaris et al., 2003; Huang and Riggs, 2000; Senjanovic et al., 2008b, 2008a). It would be interesting to apply such methods to model ice floes.

This paper presents a solution for a two-dimensional ice floe of variable properties using the generalized-mode method. The outline is as follows. In Section 2 we present a solution method for the case of

* Corresponding author.
E-mail addresses: smith@math.auckland.ac.nz (M.J.A. Smith), meylan@math.auckland.ac.nz (M.H. Meylan).

0165-232X/$ – see front matter © 2011 Elsevier B.V. All rights reserved.
doi:10.1016/j.coldregions.2011.03.003

an ice floe of uniform properties by expanding in terms of the free modes. This solution is presented very carefully and we explain each step in the solution, although this method has appeared in other papers (as discussed previously). In Section 3 we then show how we can calculate the solution for a plate of variable properties very simply, from the solution for a plate of uniform properties. In Section 4 we present some results which focus on the effect of variable properties including realistic variations in floe thickness. Section 5 is a summary.

2. Solution for a uniform ice floe

We begin with the problem of a one-dimensional uniform ice floe, modeled as an elastic plate, floating on the surface of a fluid of constant finite depth h. A two-dimensional solution for the problem in the vertical xz plane is found. The solution we present here is closely related to the generalized-mode solution presented by Newman (1994). We will show in the following section how this solution can be modified for the case of a non-uniform ice floe. In our particular case, we use regular cartesian coordinates with the z-axis vertically up, and the x-axis in the direction of the water surface.

2.1. Equations in the time domain

We assume that the fluid flow is irrotational and inviscid, and we linearize all equations. The equations for the fluid are as follows:

$$\Delta\Phi = 0, -h<z<0, \tag{1a}$$

$$\partial_z\Phi = 0,\ z = -h, \tag{1b}$$

$$\partial_z\Phi = \partial_t\eta,\ z = 0, \tag{1c}$$

$$-\rho\partial_t\Phi - \rho g\eta = P,\ z = 0, \tag{1d}$$

where Φ is the velocity potential for the fluid, η is the displacement of the free surface, ρ is the fluid density, g is the acceleration due to gravity, and P is the pressure. Note that Eq. (1a) is Laplace's equation for an irrotational, inviscid medium, Eq. (1b) is the condition that there is no flow through the seabed, Eq. (1c) is the kinematic condition and Eq. (1d) is the dynamic condition for the plate.

We assume that the pressure is zero, except under the floe which occupies the region $-L\leq x\leq L$. Under the floe the dynamic condition is

$$D\partial_x^4\eta + m\partial_t^2\eta = -\rho\partial_t\Phi - \rho g\eta, x\in(-L,L),\ z = 0, \tag{2}$$

where D is the stiffness of the plate and $m=\rho_i d$ is the mass per unit length (ρ_i is the density of the floe and d is the floe thickness). We also have conditions at the ends of the floe, which are assumed free. The free conditions are

$$\partial_x^2\eta = \partial_x^3\eta = 0, x = \pm L. \tag{3}$$

2.2. Non-dimensionalization and transformation to the frequency domain

We non-dimensionalize all lengths with respect to a length parameter L (which we keep as arbitrary) and time with respect to $\sqrt{L^*/g}$ (so that gravity is unity). We now consider the equations in the frequency domain and assume that all time-varying quantities are proportional to $e^{i\omega t}$, so that we can write

$$\eta(x,t) = Re\left\{\zeta e^{i\omega t}\right\}, \tag{4a}$$

$$\Phi(x,t) = Re\left\{\phi e^{i\omega t}\right\}. \tag{4b}$$

Under this assumption, Eqs. (1) and (2) become

$$\Delta\phi = 0, -h<z<0, \tag{5a}$$

$$\partial_z\phi = 0, z = -h, \tag{5b}$$

$$\partial_z\phi = \alpha\phi, x\notin(-L,L), z = 0, \tag{5c}$$

$$\partial_z\phi = i\omega\zeta, x\in(-L,L), z = 0, \tag{5d}$$

$$\beta\partial_x^4\zeta + (1-\gamma\alpha)\zeta = -i\omega\phi, x\in(-L,L), z = 0, \tag{5e}$$

where $\alpha=\omega^2$, $\beta=D/\rho g L^4$, $\gamma=m/\rho L$, and all variables have been converted to their non-dimensional equivalents. The edge condition (3) also apply.

2.3. Boundary conditions at $x\to\pm\infty$

Eqs. (5a)–(5e) also require boundary conditions as $x\to\pm\infty$. We choose these to be an incident wave of unit amplitude (in potential) incoming from $x\to-\infty$, plus corresponding reflected and transmitted waves. These imply that

$$\lim_{x\to-\infty}\phi = \frac{\cosh(k(z+h))}{\cosh(kh)}e^{-ikx} + R\frac{\cosh(k(z+h))}{\cosh(kh)}e^{ikx}, \tag{6}$$

where k is the positive real solution of the dispersion relation $k\tanh(kh)=\alpha$, and R is the reflection coefficient. We also have

$$\lim_{x\to\infty}\phi = T\frac{\cosh(k(z+h))}{\cosh(kh)}e^{-ikx}, \tag{7}$$

where T is the transmission coefficient.

2.4. Modes of vibration for a uniform plate

We now expand the displacement of the floe in terms of the modes of vibration of a free plate, which satisfy

$$\partial_x^4 X_n = \mu_n^4 X_n, \tag{8}$$

and the free-edge conditions

$$\partial_x^2 X_n = \partial_x^3 X_n = 0, x = \pm L. \tag{9}$$

These modes are given by

$$X_0 = \frac{1}{\sqrt{2L}}, \tag{10a}$$

$$X_1 = \sqrt{\frac{3}{2L^3}}x, \tag{10b}$$

$$X_{2n}(x) = \frac{1}{\sqrt{2L}}\left(\frac{\cos(\mu_{2n}x)}{\cos(\mu_{2n}L)} + \frac{\cosh(\mu_{2n}x)}{\cosh(\mu_{2n}L)}\right), \tag{10c}$$

and

$$X_{2n+1}(x) = \frac{1}{\sqrt{2L}}\left(\frac{\sin(\mu_{2n+1}x)}{\sin(\mu_{2n+1}L)} + \frac{\sinh(\mu_{2n+1}x)}{\sinh(\mu_{2n+1}L)}\right), \tag{10d}$$

where $\mu_0 = \mu_1 = 0$, and μ_n for $n \geq 2$ are the roots of

$$(-1)^n \tan(\mu_n L) + \tanh(\mu_n L) = 0. \tag{10e}$$

Note that we have defined the plate eigenfunctions so that they satisfy the following normalizing condition

$$\int_{-L}^{L} X_m(x) X_n(x) dx = \delta_{mn}, \tag{11}$$

where δ_{mn} is the Kronecker delta. We expand the displacement of the floe in terms of the modes, and obtain

$$\zeta = \sum_{n=0}^{N} \zeta_n X_n. \tag{12}$$

2.5. Radiated, diffracted, and incident potential

We substitute the expansion of the displacement of the floe in terms of modes (12) into Eqs. (5a) to (5d), and we obtain the following equations for the potential

$$\Delta\phi = 0, -h<z<0, \tag{13a}$$

$$\partial_z \phi = 0,\ z = -h, \tag{13b}$$

$$\partial_z \phi = \alpha\phi, x \notin (-L, L),\ z = 0, \tag{13c}$$

$$\partial_z \phi = i\omega \sum_{n=0}^{N} \zeta_n X_n,\ x \in (-L, L),\ z = 0. \tag{13d}$$

From linearity, the potential can be written as

$$\phi = \phi^D + \sum_{n=0}^{N} \zeta_n \phi_n^R, \tag{14}$$

where ϕ^{D} is the diffracted potential and ϕ_n^{R} are the radiated potentials. The diffracted potential satisfies

$$\Delta\phi^{\mathrm{D}} = 0, -h<z<0, \tag{15a}$$

$$\partial_z \phi^{\mathrm{D}} = 0, z = -h, \tag{15b}$$

$$\partial_z \phi^{\mathrm{D}} = \alpha\phi^{\mathrm{D}}, x \notin (-L, L), z = 0, \tag{15c}$$

$$\partial_z \phi^{\mathrm{D}} = 0, x \in (-L, L), z = 0, \tag{15d}$$

and the Sommerfeld radiation condition

$$\frac{\partial}{\partial x}\left(\phi^{\mathrm{D}} - \phi^{\mathrm{I}}\right) \pm \mathrm{i}k\left(\phi^{\mathrm{D}} - \phi^{\mathrm{I}}\right) = 0, \text{as } x \to \pm\infty, \tag{16}$$

where ϕ^{I} is the incident potential given by

$$\phi^{\mathrm{I}} = \frac{\cosh(k(z+h))}{\cosh(kh)} e^{-ikx}. \tag{17}$$

The radiation potentials satisfy the following equations

$$\Delta\phi_n^R = 0, -h<z<0, \tag{18a}$$

$$\partial_z \phi_n^R = 0,\ z = -h, \tag{18b}$$

$$\partial_z \phi_n^{\mathrm{R}} = \alpha\phi_n^{\mathrm{R}},\ x \notin (-L, L),\ z = 0, \tag{18c}$$

$$\partial_z \phi_n^{\mathrm{R}} = \mathrm{i}\omega X_n,\ x \in (-L, L),\ z = 0, \tag{18d}$$

and the Sommerfeld radiation condition

$$\frac{\partial \phi_n^{\mathrm{R}}}{\partial x} \pm ik\phi_n^{\mathrm{R}} = 0, \text{as } x \to \pm\infty. \tag{19}$$

2.6. Solution for the radiation and diffracted potential using Green's function

We solve for the diffracted and radiation potentials using Green's function, which for our case is required to only have a singularity at the surface, since we are neglecting the submergence of the floe. Green's function is therefore given by the following system of equations

$$\Delta G(\mathbf{x}, \xi) = 0, -h<z<0, \tag{20a}$$

$$\partial_z G - \alpha G = \delta(x - \xi), z = 0, \tag{20b}$$

$$\partial_z G = 0, z = -h, \tag{20c}$$

(plus the Sommerfeld radiation condition of no incoming waves) where $\mathbf{x} = (x, z)$ and $\xi = (\xi, \eta)$. We can write the solution for Green's function as

$$G(x, \xi) = \sum_{n=0}^{N} -\frac{e^{-k_n|x-\xi|}}{\tan(k_n h) + hk_n \sec^2(k_n h)}, \tag{21}$$

where k_n are the solutions of the dispersion equation

$$\alpha = -k_n \tan(k_n h), \tag{22}$$

with k_0 being the first pure imaginary root, with positive imaginary part ($k_0 = \mathrm{i}k$), and k_n being the positive real roots ordered by increasing size, for $n \geq 1$ (Linton and McIver, 2002).

We then use Green's second identity to obtain the following integral equations for the radiated and diffracted potentials,

$$\phi^{\mathrm{D}}(x) = \phi^{\mathrm{I}}(x) + \int_{-L}^{L} G(x, \xi)\alpha\phi^{\mathrm{D}}(\xi) d\xi, \tag{23}$$

and

$$\phi_n^{\mathrm{R}}(x) = \int_{-L}^{L} G(x, \xi)\left(\alpha\phi_n^{\mathrm{R}}(\xi) - \mathrm{i}\omega X_n(\xi)\right)\ d\xi, \tag{24}$$

which we solve by standard integral equation methods.

2.7. Solution for the floe

If we substitute the solution for the radiated and diffracted potential into Eq. (5e), we obtain

$$\sum_{n=0}^{N} \left(\beta\mu_n^4 - \alpha\gamma + 1\right)\zeta_n X_n = -\mathrm{i}\omega\left(\phi^{\mathrm{D}} + \sum_{n=0}^{N} \zeta_n \phi_n^{\mathrm{R}}\right). \tag{25}$$

If we then multiply by X_m and integrate over the wetted surface, we obtain

$$\sum_{n=0}^{N} \left(\left(\mu_n^4 - \alpha\gamma + 1\right)\right)\zeta_n = -\mathrm{i}\omega\left(\int_{-L}^{L} \phi^{\mathrm{D}} X_m \mathrm{d}x + \sum_{n=0}^{N} \zeta_n \int_{-L}^{L} \phi_n^{\mathrm{R}} X_m \mathrm{d}x\right). \tag{26}$$

We now introduce the following notation. We define the diagonal matrices $\mathbf{K}$ and $\mathbf{M}$ by the elements

$$\mathbf{K}_{mm} = \beta\mu_m^4, \tag{27}$$

$$\mathbf{M}_{mm} = \gamma, \tag{28}$$

which are the stiffness and mass matrices respectively for this problem. The hydrostatic restoring matrix **C** is the identity matrix for this problem, that is, **C** = **I**. The added mass matrix **A** and damping matrix **B** are given by

$$-\alpha \mathbf{A}_{mn} + i\omega \mathbf{B}_{mn} = i\omega \int_{-L}^{L} \phi_n^{\mathrm{R}}(x) X_m(x) \mathrm{d}x. \tag{29}$$

We also define the vector **f** by the elements

$$f_n = \int_{-L}^{L} \phi^{\mathrm{D}} X_n \ \mathrm{d}x. \tag{30}$$

Then we can write Eq. (26) as

$$(\mathbf{K} - \alpha \mathbf{M} + \mathbf{C} - \alpha \mathbf{A} + i\omega \mathbf{B}) \vec{\zeta} = \mathbf{f}. \tag{31}$$

This equation is analogous to the equation in modes for a rigid-body (in which case the stiffness matrix **K** is zero).

2.8. Reflection and transmission coefficients

The reflection coefficient can be found using Green's second identity with the solution potential ϕ, and ϕ^{I}, to obtain

$$R = -\frac{1}{(\tan(k_0 h) + k_0 h \sec(k_0 h)^2)} \int_{-L}^{L} e^{-ikx} (\alpha \phi(x) - \partial_n \phi(x)) \ \mathrm{d}x. \tag{32}$$

Similarly, if we use a wave incident from $x \to \infty$, we obtain the transmission coefficient

$$T = 1 - \frac{1}{(\tan(k_0 h) + k_0 h \sec(k_0 h)^2)} \int_{-L}^{L} e^{ikx} (\alpha \phi(x) - \partial_n \phi(x)) \ \mathrm{d}x. \tag{33}$$

3. Non-uniform free floe

We now show how the solution for a uniform floe can be extended to a solution for a floe of variable properties. In the case of a non-uniform floe, the Euler–Bernoulli plate equation is

$$\partial_x^2 \left(\beta(x) \partial_x^2 \zeta \right) + \gamma(x) \partial_t^2 \zeta = 0, \tag{34}$$

plus the edge condition (3). We denote the eigenfunctions for the non-uniform plate equation by $\hat{X}_{n,}$, and the corresponding eigenvalues by $\hat{\mu}_n$. They satisfy

$$\partial_x^2 \left(\beta(x) \partial_x^2 \hat{X}_n \right) = \gamma(x) \hat{\mu}_n^4 \hat{X}_n. \tag{35}$$

These eigenfunctions are the stationary points of the following variational problem

$$J[\zeta] = \frac{1}{2} \int_{-L}^{L} \left\{ \beta(x) \left(\partial_x^2 \zeta \right)^2 - \hat{\mu}^4 \gamma(x) \zeta^2 \right\} \mathrm{d}x, \tag{36}$$

(which is based on a similar expression from (Lanczos, 1949)) where $\hat{\mu}^4$ is also the Lagrange multiplier. We can find these eigenfunctions using the Rayleigh–Ritz method by expanding in terms of the eigenfunctions for a free plate. We write

$$\hat{X}_m \approx \sum_{n=0}^{N} q_{mn} X_n(x), \tag{37}$$

and we find q_{mn} by solving the following generalized eigenvalue equation

$$\mathcal{K} \mathbf{q}_m = \mu_m \mathcal{M} \mathbf{q}_m, \tag{38}$$

where the elements of the matrices $\mathcal{K}$ and $\mathcal{M}$ are given by

$$\mathcal{K}_{mn} = \int_{-L}^{L} \beta(x) X_m'' X_n'' \ \mathrm{d}x, \tag{39a}$$

$$\mathcal{M}_{mn} = \int_{-L}^{L} \gamma(x) X_m X_n \ \mathrm{d}x. \tag{39b}$$

Note that we have an exact representation of X_n so these integrals can be performed with as much accuracy as needed. Also, the notation is chosen to reflect that matrices K and M are also referred to as the mass and stiffness matrices. We define the matrix **Q** as the matrix with elements given by q_{mn}.

3.1. Equations for a non-uniform floe

The equations for a non-uniform floe are virtually the same as those given for a uniform floe (5a) to (5e). They are

$$\Delta \phi = 0, -h < z < 0, \tag{40a}$$

$$\partial_z \phi = 0, \ z = -h, \tag{40b}$$

$$\partial_z \phi = \alpha \phi, x \notin (-L, L), \ z = 0, \tag{40c}$$

$$\partial_z \phi = i\omega \zeta, x \in (-L, L), \ z = 0, \tag{40d}$$

$$\partial_x^2 \left(\beta(x) \partial_x^2 \zeta \right) - (\gamma(x)\alpha - 1)\zeta - \alpha \phi = 0, x \in (-L, L), \ z = 0. \tag{40e}$$

As before we expand the displacement in terms of the modes, this time using the modes for the non-uniform plate. We therefore write

$$\zeta = \sum_{n=0}^{N} \hat{\zeta}_n \hat{X}_n. \tag{41}$$

From linearity, the potential can therefore be written as

$$\phi = \phi^{\mathrm{D}} + \sum_{n=0}^{N} \hat{\zeta}_n \hat{\phi}_n^{\mathrm{R}}, \tag{42}$$

where we can express the radiated potentials for the non-uniform floe in terms of the uniform floe as

$$\hat{\phi}_m^{\mathrm{R}} = \sum_{n=0}^{N} q_{mn} \phi_n^{\mathrm{R}}. \tag{43}$$

If we substitute the expansion for the displacement and potential into Eq. (40e) we obtain

$$\sum_{n=0}^{N} \left(\hat{\mu}_n^4 \gamma(x) - \gamma(x)\alpha + 1 \right) \hat{\zeta}_n \hat{X}_n = -i\omega \left(\phi^{\mathrm{D}} + \sum_{n=0}^{N} \hat{\zeta}_n \hat{\phi}_n^{\mathrm{R}} \right), \tag{44}$$

$x \in (-L, L), \ z = 0.$

If we now multiply by $\hat{X}_m$ and integrate from $-L$ to L, we obtain

$$\begin{aligned} &\sum_{n=0}^{N} \left(\hat{\mu}_n^4 - \alpha \right) \left(\int_{-L}^{L} \gamma(x) \hat{X}_m \hat{X}_n \, \mathrm{d}x \right) \hat{\zeta}_n - \sum_{n=0}^{N} \left(\int_{-L}^{L} \hat{X}_m \hat{X}_n \, \mathrm{d}x \right) \hat{\zeta}_n \\ &\quad = i\omega \left(\int_{-L}^{L} \phi^{\mathrm{D}} \hat{X}_m \, \mathrm{d}x + \sum_{n=0}^{N} \hat{\zeta}_n \int_{-L}^{L} \hat{\phi}_n^{\mathrm{R}} \hat{X}_m \, \mathrm{d}x \right). \end{aligned} \tag{45}$$

Substituting the expansion for $\hat{X}_n$ at Eq. (37), we obtain the following equation

$$\left(\hat{\mathbf{K}} - \alpha \hat{\mathbf{M}} + \hat{\mathbf{C}} - \alpha \hat{\mathbf{A}} + i\omega \hat{\mathbf{B}} \right) \hat{\zeta} = \hat{\mathbf{f}}. \tag{46}$$

where $\hat{\xi}$ is the vector formed from $\hat{\xi}_n$. In terms of the matrices defined previously we have

$$\hat{\mathbf{K}} = \lceil \hat{\mu}_n^4 \rfloor \mathbf{Q}\mathcal{M}\mathbf{Q}^{\mathrm{T}}, \tag{47a}$$

where $\lceil \ldots \rfloor$ denotes a diagonal matrix,

$$\hat{\mathbf{M}} = \mathbf{Q}\mathcal{M}\mathbf{Q}^{\mathrm{T}}, \tag{47b}$$

$$\hat{\mathbf{C}} = \mathbf{Q}\mathbf{C}\mathbf{Q}^{\mathrm{T}}, \tag{47c}$$

$$\hat{\mathbf{A}} = \mathbf{Q}\mathbf{A}\mathbf{Q}^{\mathrm{T}}, \tag{47d}$$

$$\hat{\mathbf{B}} = \mathbf{Q}\mathbf{B}\mathbf{Q}^{\mathrm{T}}, \tag{47e}$$

$$\hat{\mathbf{f}} = \mathbf{Q}\mathbf{f}. \tag{47f}$$

Note that further simplifications are possible, for example we know from before that $\mathbf{C} = \mathbf{I}$, but to illustrate the general connection this has not been done here. Also, the matrix of eigenfunction $\mathbf{Q}$ can be normalized so that $\hat{\mathbf{M}}$ is the identity matrix. The reflection and transmission coefficients are determined exactly as before.

4. Results

In what follows we consider the ice floes to have Young's modulus $E = 6 \times 10^9$ Pa, Poisson's ratio $\nu = 0.3$, $\rho_w = 1000$, and $\rho_i = 900$. We begin by considering some ice floes with very simple (and unrealistic) variations in thickness. We consider four shapes for the thickness which we denote by $g_n(x)$ which are shown in Fig. 1. Note that all four functions have the same average thickness. The thickness for the floe will be given by $d_n(x) = d_0 g_n(x)$. Note that the floe has length of $2L = 200$ m.

Figs. 2 and 3 show the effect on the reflection and transmission coefficients for the four shapes for the values of d_0 shown. Figs. 4 and 5 are the same curves as in Figs. 2 and 3, but this time the figures are grouped by shape. These figures show that the qualitative behaviour of the plate is not strongly affected by the exact distribution of thickness for the floe, but that the values of thickness have a very strong effect. However, as the thickness becomes smaller the effect of variable thickness does show some significance. This effect is investigated in more detail by comparison to realistic variations in ice floe thickness.

The results so far have been for simple variations in ice floe thickness. In practice the real ice floe thickness will follow a complicated random function. Instead of trying to simulate this variation, we consider here ice floes which vary according to measured ice thickness. The ice thickness variations we consider here are given by the *National Snow and Ice Data Center* measured in the Arctic. We have taken the results from four of the SCICEX-99 data set collected on 2 April 1999 (numbers 402.003.001, 402.004.001, 402.004.002, and 402.005.001 in the NSIDC numbering). We take these as representative of typical ice floe thickness variations in the absence of better data. We scale these actual measurements so that the average thickness has a prescribed value. Fig. 6 shows the thickness for three random floes of length 100 m taken from a sample whose average floe thickness is 0.5 m over this entire sample. This figure gives an idea of typical values for the variation in floe thickness and shows clearly that each floe does not have average thickness exactly 0.5 m although the thickness varies around this value.

Since the floe thickness is now a random variable, we present average values for the scattering. Fig. 7 shows the absolute value of the reflection coefficient versus period for floes of length 2 L equals 50 m, 100 m, 200 m, and 400 m The average thickness is 0.5 m. Note that this is the average over the sample and does not mean that each floe had average thickness 0.5 m. The dashed curve is the solution for a uniform floe. Fig. 8 is the equivalent results for floes of thickness 1 m. These results show that the random thickness has only a small effect

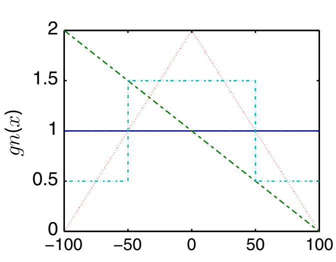

Fig. 1. The shapes $g_n(x)$ used for the floe thickness $d(x)$. The solid line is $g_1(x)$, the dashed line is $g_2(x)$, the dotted line is $g_3(x)$, and the chained line is $g_4(x)$.

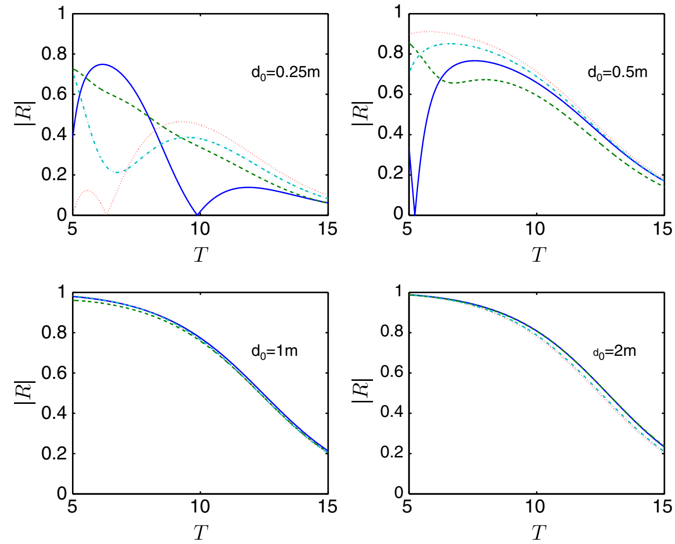

Fig. 2. The reflection coefficient $|R|$ versus period T for thickness $d(x) = d_0 g_n(x)$ for the values of d_0 shown. The solid line is shape $g_1(x)$, the dashed line is shape $g_2(x)$, the dotted line is shape $g_3(x)$, and the chained line is shape $g_4(x)$.

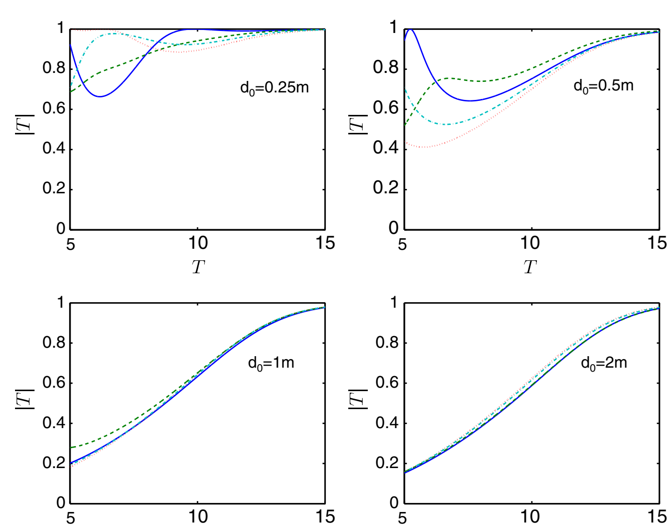

Fig. 3. As in Fig. 2 except that we plot the transmission coefficient $|T|$.

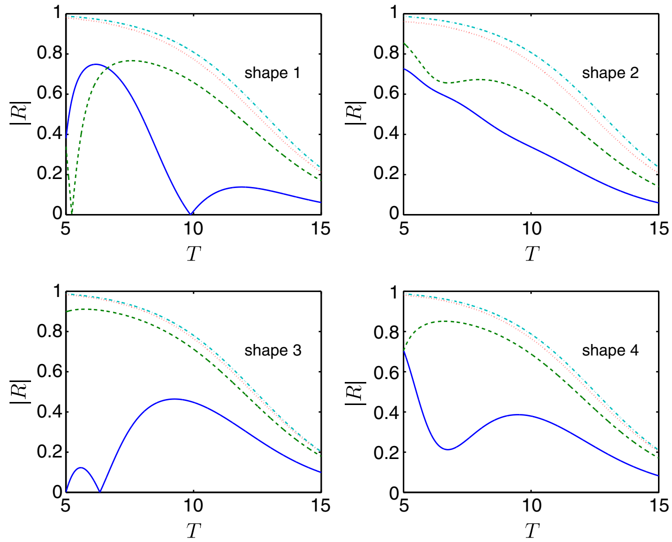

Fig. 4. The reflection coefficient $|R|$ versus period T, for thickness $d(x) = d_0 g_n(x)$ for four values of d_0. The solid line is $d_0 = 0.25$ m, the dashed line is $d_0 = 0.5$ m, the dotted line is $d_0 = 1$ m, and the chained line is $d_0 = 2$ m.

for short floes and a strong effect for large floes. The transition from short to large occurs at greater lengths as the floe thickness increases and seems to be independent of period. We suggest that this variable floe thickness become more important for longer floes because of the greater importance of bending for longer floes. We also note that the effect of random thickness seems to reduce the reflection (and increase the transmission). However, in all cases they are the same order of magnitude. We also note that the effect of floe size is much more important when the random variation in thickness is included and that the effect of floe length is of similar importance to that of floe thickness.

5. Summary

We have shown how the solution for an ice floe of variable properties can be found from the equivalent solution for an ice floe of uniform properties, with minor modifications of the solution method. The methods rely on an expansion of the modes of vibration for a non-uniform plate in terms of the uniform plate modes, which is accomplished using the Rayleigh–Ritz method. This allows us to then use the solution for the added mass and damping matrices for the uniform floe to find the solution for the non-uniform floe. Various results were presented showing the effect of variable floe thickness. The inclusion of variable thickness could have some effect on the scattering of waves by ice floes, although it is not going to make an order of magnitude difference, or equivalent for quantities such as the total scattering.

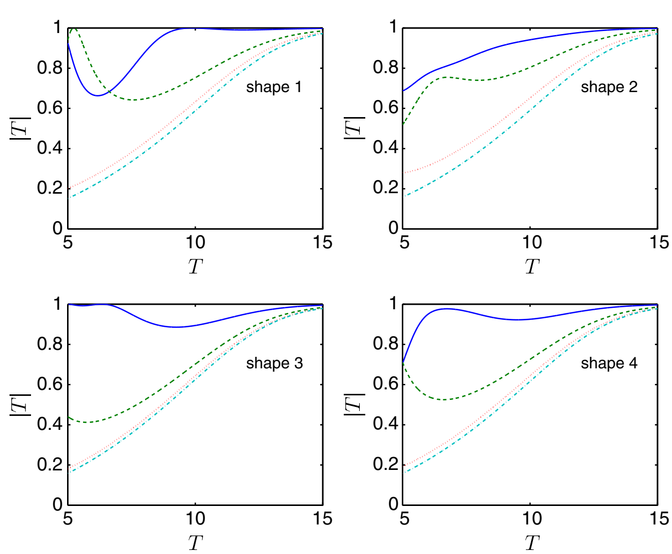

Fig. 5. As in Fig. 4 except that we plot the transmission coefficient $|T|$.

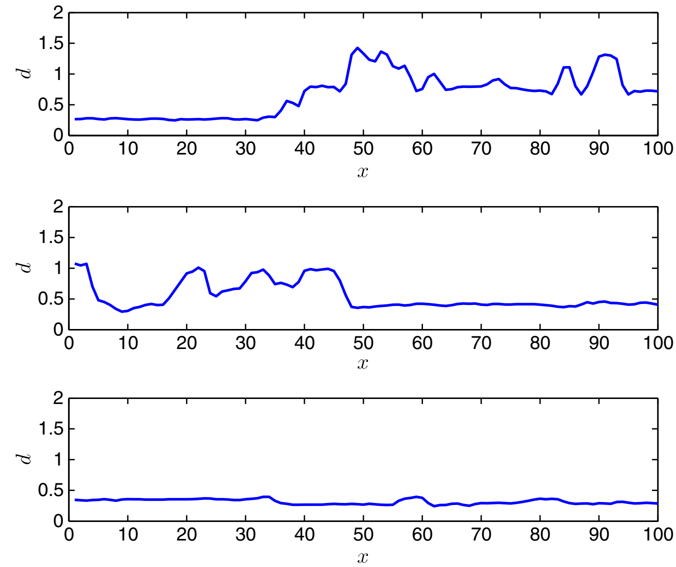

Fig. 6. The thickness $d(x)$ along the length of a floe for three typical random floes. The floe length is 100 m and the thickness is chosen from a sample with average thickness of 0.5 m.

Acknowledgements

The numerical code to solve the dispersion equations was provided by Tim Williams. The authors would also like to thank Dr. Garry Tee for his careful reading of the manuscript. The data used

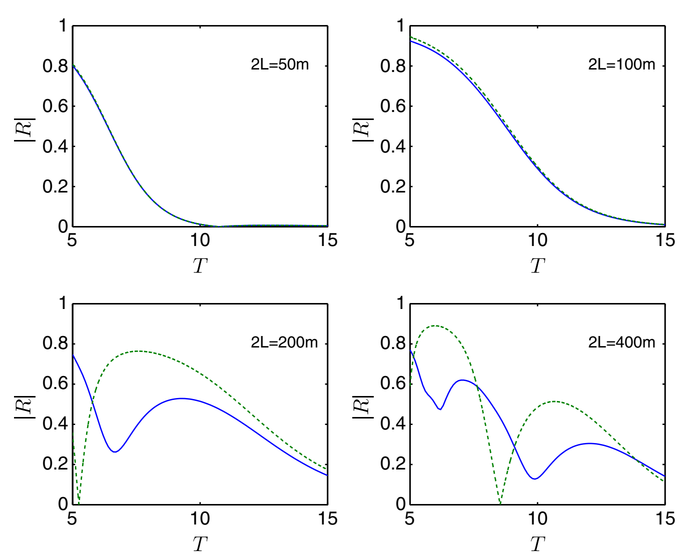

Fig. 7. The reflection coefficient $|R|$ versus period T for ice floes of lengths as shown with the solid line being the average for random floe thickness with mean 0.5 m and the dashed line being the result for a floe of uniform thickness 0.5 m.

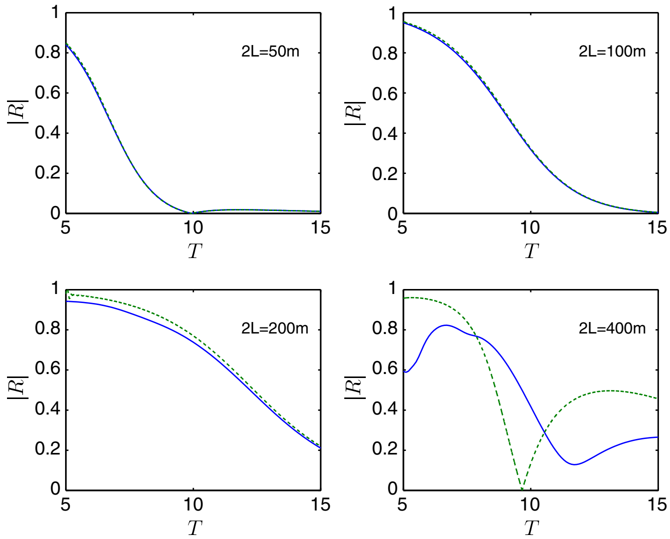

Fig. 8. As in Fig. 7 except that the thickness is 1 m.

to determine realistic ice floe thickness was taken from the National Snow and Ice Data Center.

References

Balmforth, N., Craster, R., 1999. Ocean waves and ice sheets. J. Fluid Mech. 395, 89–124.
Bennetts, L.G., Biggs, N.R.T., Porter, D., 2009. Wave scattering by multiple rows of circular ice floes. J. Fluid Mech. 639, 213–238.
Chung, H., Fox, C., 2002. Calculation of wave–ice interaction using the Wiener–Hopf technique. NZ J. Math. 31, 1–18.
Fox, C., Squire, V.A., 1994. On the oblique reflexion and transmission of ocean waves at shore fast sea ice. Phil. Trans. R. Soc. Lond. A. 347, 185–218.
Hazard, C., Meylan, M.H., 2007. Spectral theory for a two-dimensional elastic thin plate floating on water of finite depth. SIAM J. Appl. Math. 68 (3), 629–647.
Hirdaris, S.E., Price, W.G., Temarel, P., 2003. Two- and three-dimensional hydroelastic modelling of a bulker in regular waves. Mar. struct. 16, 627–658.
Huang, L.L., Riggs, R.R., 2000. The hydrostatic stiffness of flexible floating structure for linear hydroelasticity. Mar. struct. 13, 91–106.
Kohout, A.L., Meylan, M.H., 2009. Wave scattering by multiple floating elastic plates with spring or hinged boundary conditions. Mar. struct. 22, 712–729.
Kohout, A.L., Meylan, M.H., Sakai, S., Hanai, K., Leman, P., Brossard, D., 2007. Linear water wave propagation through multiple floating elastic plates of variable properties. J. Fluids Struct. 23 (4), 649–663.
Lanczos, C. (Ed.), 1949. The Variational Principles of Mechanics. University of Toronto Press, Toronto.
Linton, C.M., McIver, M., 2002. The existence of Rayleigh–Bloch surface waves. J. Fluid Mech. 470, 85–90.
Mahmood-ul-Hassan, Meylan, M.H., Peter, M.A., 2009. Water-wave scattering by submerged elastic plates. Quart. J. Mech. Appl. Math. 62 (3), 321–344.
Mei, C.C., 1989. The Applied Dynamics of Ocean Surface Waves. World Scientific.
Meylan, M.H., Squire, V.A., 1994. The response of ice floes to ocean waves. J. Geophys. Res. 99 (C1), 891–900.
Meylan, M.H., Sturova, I.V., 2009. Time-dependent motion of a two-dimensional floating elastic plate. J. Fluids Struct. 25 (3), 445–460.
Newman, J.N., 1977. Marine Hydrodynamics. MIT Press.
Newman, J.N., 1994. Wave effects on deformable bodies. Appl. Ocean Res. 16, 45–101.
Peter, M.A., Meylan, M.H., Chung, H., 2004. Wave scattering by a circular elastic plate in water of finite depth: a closed form solution. IJOPE 14 (2), 81–85.
Senjanovic, I., Malenica, S., Tomasevic, S., 2008a. Hydroelasticity of large container ships. Mar. struct. 22 (2), 287–314.
Senjanovic, I., Malenica, S., Tomasevic, S., 2008b. Investigation of ship hydroelasticity. Mar. struct. 35 (5–6), 523–535.
Squire, V.A., 2007. Of ocean waves and sea-ice revisited. Cold Reg. Sci. Technol. 49 (2), 110–133.
Tkacheva, L.A., 2001. Surface wave diffraction on a floating elastic plate. Fluid Dyn. 36 (5), 776–789.
Tkacheva, L.A., 2004. The diffraction of surface waves by a floating elastic plate at oblique incidence. J. Appl. Math. Mech. 68 (3), 425–436.
Wadhams, P., 1973. The effect of a sea ice cover on ocean surface waves. Ph.D. thesis, Scott Polar Research Institute, University of Cambridge.
Wadhams, P., 1986. The seasonal ice zone. In: Untersteiner, N. (Ed.), The Geophysics of Sea Ice. Plenum, New York, pp. 825–991.
Watanabe, E., Utsunomiya, T., Wang, C.M., 2004. Hydroelastic analysis of pontoon-type VLFS: a literature survey. Eng. Struct. 26 (2), 245–256.
Williams, T., Porter, R., 2009. The effect of submergence on the scattering by the interface between two semi-infinite sheets. J. Fluids Struct. 25 (5), 777–793.
Williams, T., Squire, V., 2010. On the estimation of ice thickness from scattering observations. Dyn. Atmos. Oceans 49 (2–3), 215–233.
Williams, T.D., Squire, V.A., 2004. Oblique scattering of plane flexural-gravity waves by heterogeneities in sea-ice. Proc. R. Soc. Lon. Ser A 460, 3469–3497.